Supplementary data

Effective Photocatalytic Hydrogen Evolution Using Covalent Triazine Framework-Derived Carbon Nitride Nanofiber Containing Carbon Vacancies for Visible-Light-Driven

Liangjing Zhang [1,†], Aiwu Wang [1,†], Mei Zhang [2], Zhengyuan Jin [1,*], Huan Yi [3,*] and Meng Wang [1,4,*]

[1] Shenzhen Key Laboratory of Ultraintense Laser and Advanced Material Technology, Center for Advanced Material Diagnostic Technology, Shenzhen Technology University, Shenzhen 518118, China; zhangliangjing@sztu.edu.cn (L.Z.); wangaiwu@sztu.edu.cn (A.W.)
[2] School of Materials Science and Engineering, Beijing Institute of Fashion Technology, Beijing 100029, China; 20140027@bift.edu.cn
[3] College of Science, Civil Aviation University of China, Tianjin 300300, China
[4] Sino-German College of Intelligent Manufacturing, Shenzhen Technology University, Shenzhen 518118, China

* Correspondence: jinzhengyuan@sztu.edu.cn (Z.J.); hyi@cauc.edu.cn (H.Y.); wangmeng@sztu.edu.cn (M.W.); Tel.: +86-0755-26532350 (Z.J.)
† These authors contributed equally to this work.

Contents

Figures

Fig. S1. (a, b) FTIR spectra for xH_2O-CN , 1:x CN and FCN. (c,d) FTIR spectra for xH_2O-CTF and 1:xCTF. (e,f) XRD patterns for xH_2O-CN , 1:x CN and FCN.
Fig. S2. (a-e) SEM images for 1:xCN.
Fig. S3. (a, b) SEM and the corresponding EDS images of CTF and CN.
Fig. S4. (a,b) Photocatalytic H_2 evolution of xH_2O, 1:xCN and FCN. (c, d) PL spectra for xH_2O, 1:xCN and FCN.
Fig. S5 The H_2 evolution cycling plots for CN through 24 h of operation.
Fig. S6(a) UV-vis diffuse reflectance spectra of xH_2O. (b) Plots of $(\alpha h\upsilon)^2$ vs. photon energy ($h\upsilon$) of xH_2O. (c) UV-vis diffuse reflectance spectra of 1:xCN and FCN. (d) Plots of $(\alpha h\upsilon)^2$ vs. photon energy ($h\upsilon$) of 1:xCN and FCN.

Tables

Table S1. (C3+C2) type of hexagonal COFs.

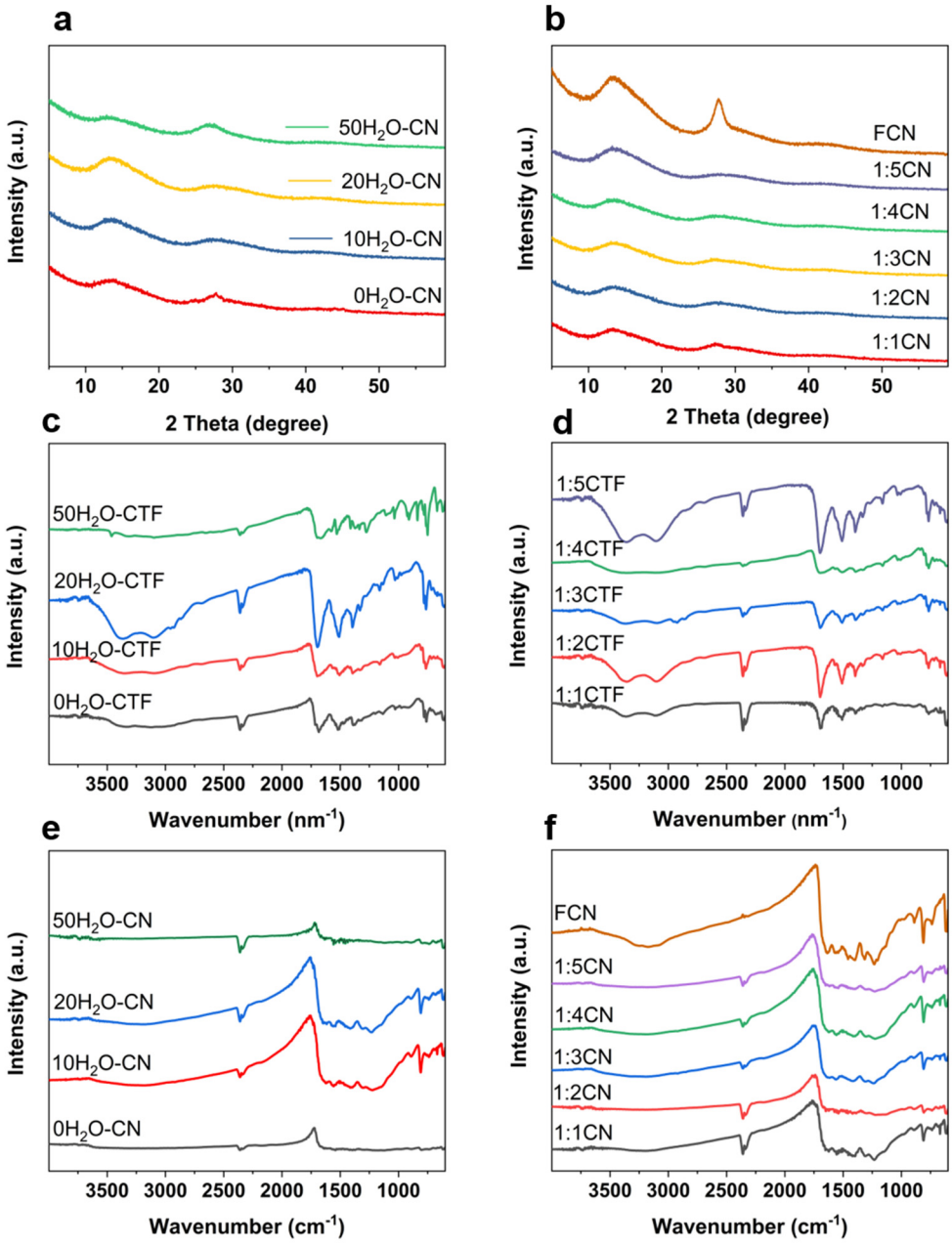

Fig. S1. (a, b) FTIR spectra for xH_2O-CN , 1:x CN and FCN. (c,d) FTIR spectra for xH_2O-CTF and 1:xCTF. (e,f) XRD patterns for xH_2O-CN , 1:x CN and FCN.

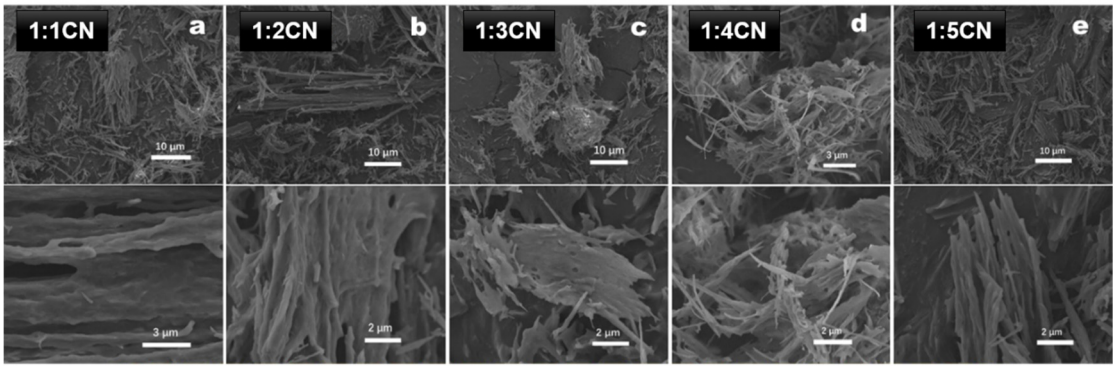

Fig. S2. (a-e) SEM images for 1:xCN.

Fig. S2 shows the effect of changing the proportions of melamine and 2,5-thiophenedicarboxylic acid on the morphology. All the samples exhibit similar fibrous morphologies, indicating that the reaction between two organic materials determines the structure of the final material. The differences in fiber thickness and number of pores result from differences in calcination duration. Higher magnification reveals a more detailed microstructure, and some fibrous structures show adhesion phenomena when viewed at higher magnifications. When the ratio between melamine and 2,5-thiophenedicarboxylic acid was 1:4, the catalyst was comprised of the smallest fibers and most porous structure. This structure facilitates the availability of a larger number of active sites in the catalytic reaction.

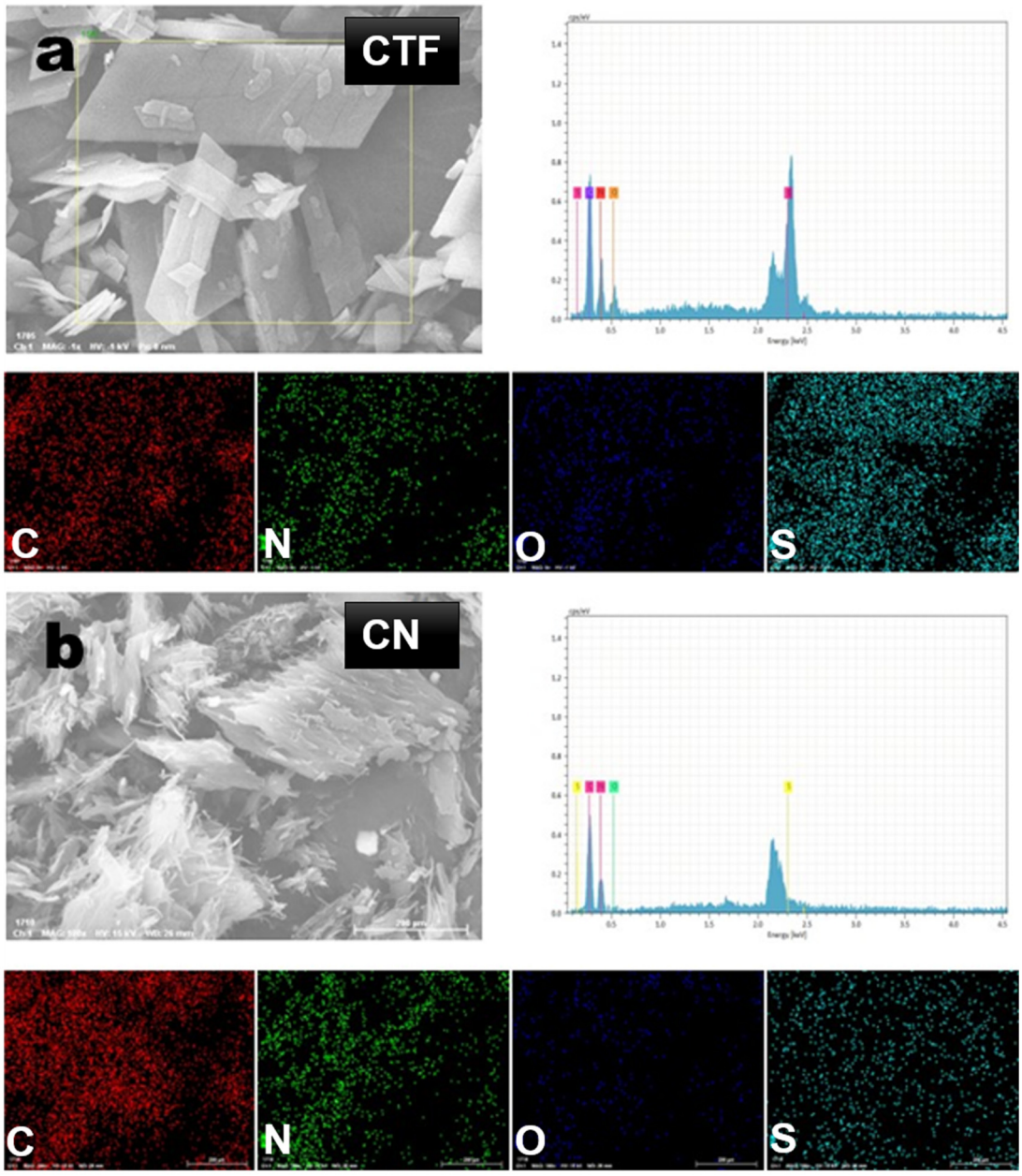

Fig. S3. (a, b) SEM and the corresponding EDS images of CTF and CN.

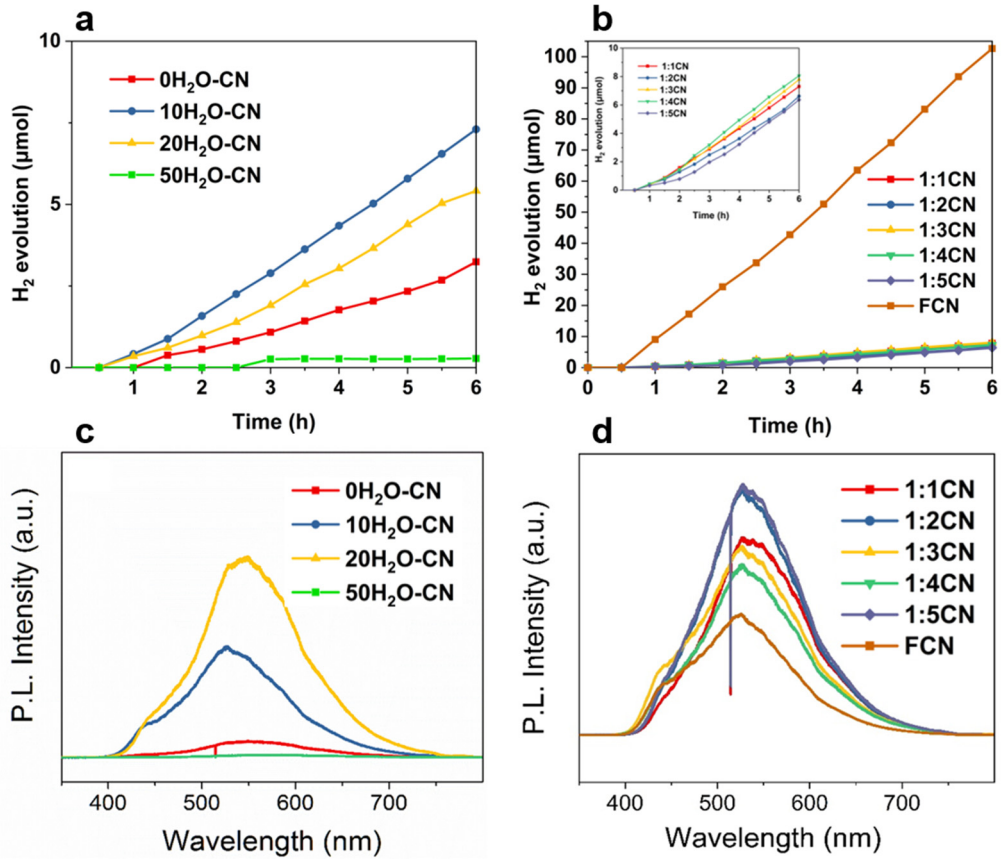

Fig. S4. (a,b) Photocatalytic H_2 evolution of xH_2O, 1:xCN and FCN. (c, d) PL spectra for xH_2O, 1:xCN and FCN.

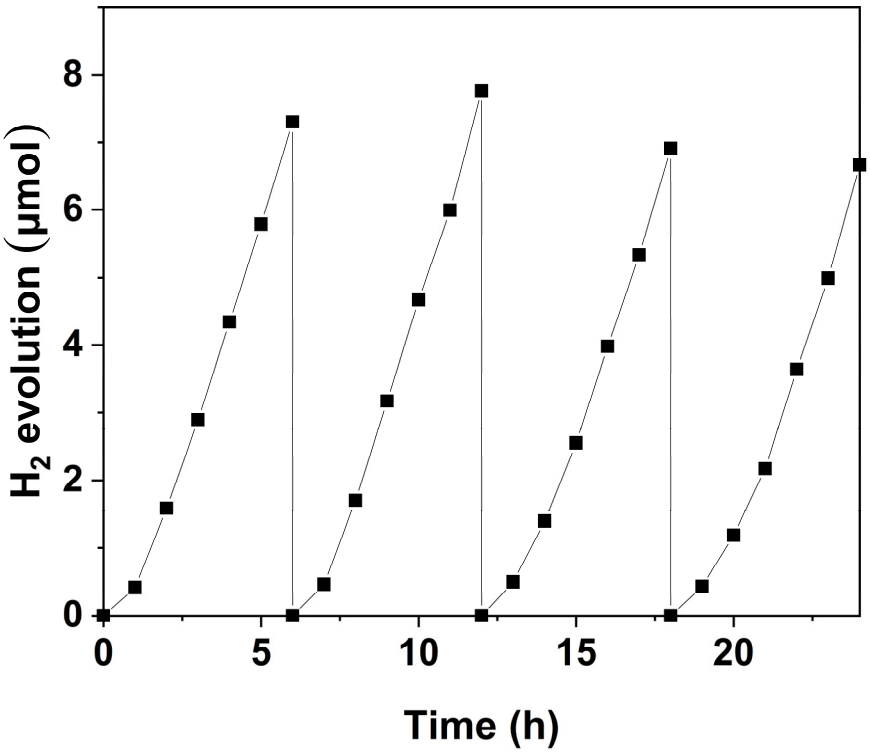

Fig. S5 The H_2 evolution cycling plots for CN through 24 h of operation.

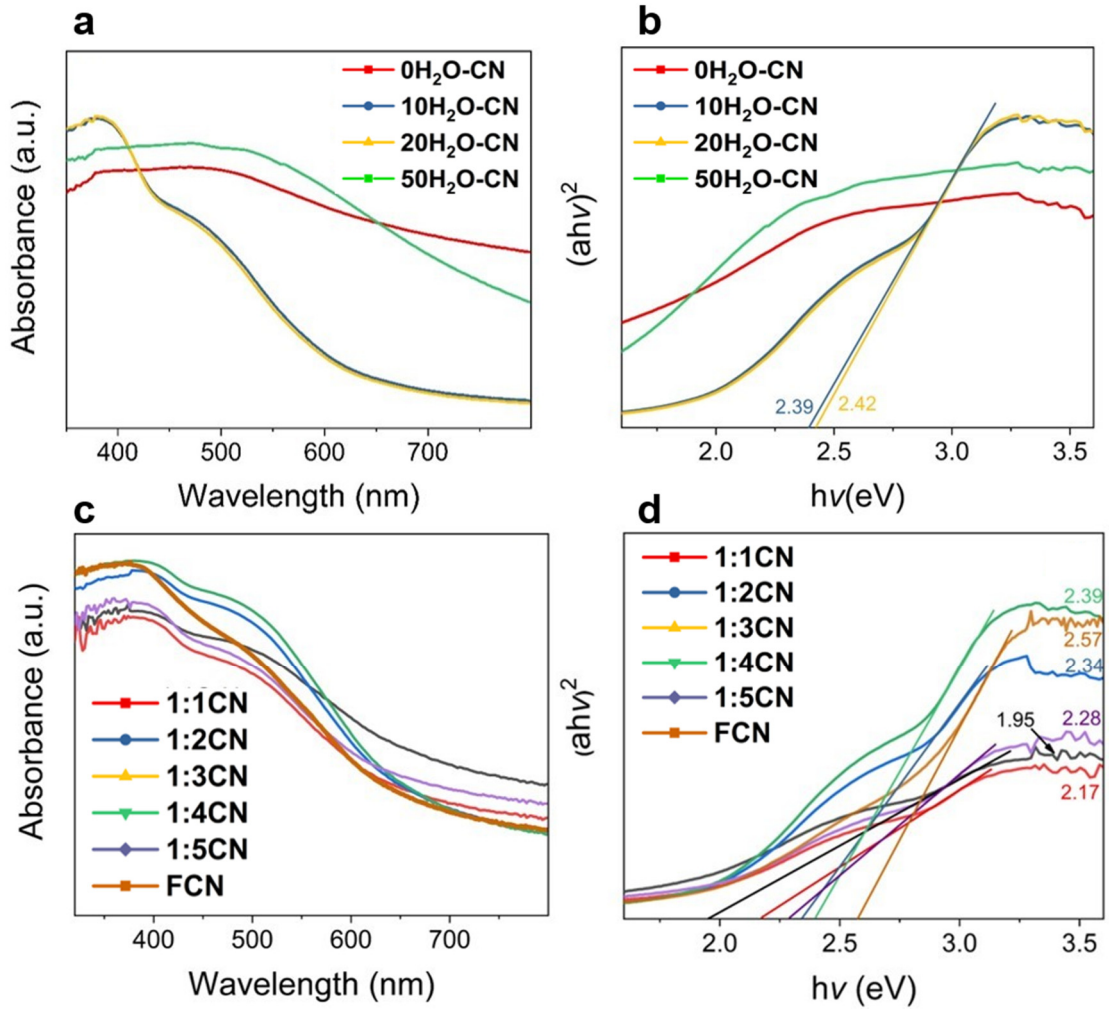

Fig. S6(a) UV-vis diffuse reflectance spectra of xH_2O. (b) Plots of $(\alpha h\upsilon)^2$ vs. photon energy ($h\upsilon$) of xH_2O. (c) UV-vis diffuse reflectance spectra of 1:xCN and FCN. (d) Plots of $(\alpha h\upsilon)^2$ vs. photon energy ($h\upsilon$) of 1:xCN and FCN.

Table S1 (C_3+C_2) type of hexagonal COFs

C_3-symmetric knots	C_2-symmetric linkers	COF	References
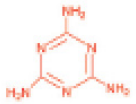	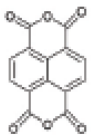	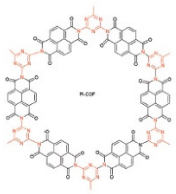	[1]
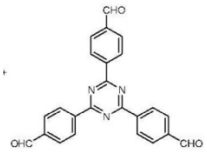	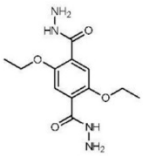	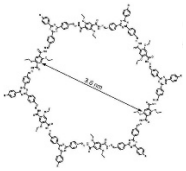	[2]
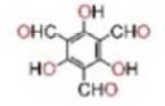		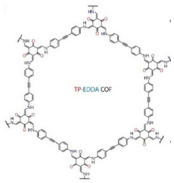	[3]
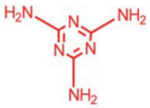	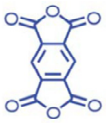	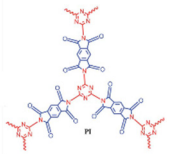	[4]
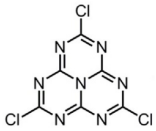	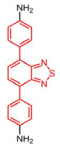	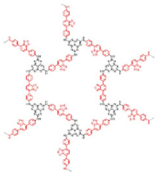	[5]
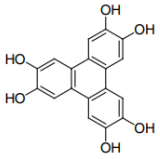	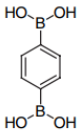	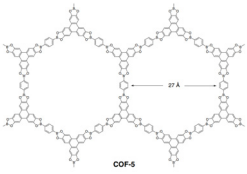	[6]
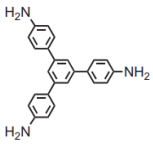	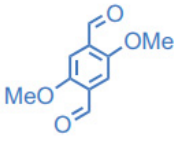	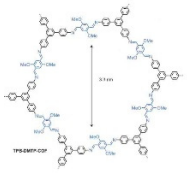	[7]
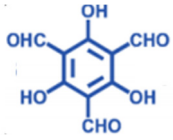	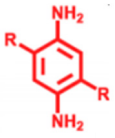	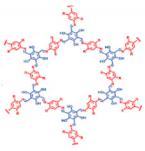	[8]

Supplementary Reference

1. Han, Y., et al., *Copper immobilized at a covalent organic framework: an efficient and recyclable heterogeneous catalyst for the Chan–Lam coupling reaction of aryl boronic acids and amines.* Green Chemistry, 2018. **20**(21): p. 4891-4900.
2. Stegbauer, L., K. Schwinghammer, and B.V. Lotsch, *A hydrazone-based covalent organic framework for photocatalytic hydrogen production.* Chem. Sci., 2014. **5**(7): p. 2789-2793.
3. Yin, H.S., et al., *Signal-on fluorescence biosensor for microRNA-21 detection based on DNA strand displacement reaction and Mg(2+)-dependent DNAzyme cleavage.* Biosens Bioelectron, 2017. **96**: p. 106-112.
4. Chu, S., et al., *Facile green synthesis of crystalline polyimide photocatalyst for hydrogen generation from water.* Journal of Materials Chemistry, 2012. **22**(31): p. 15519.
5. Kailasam, K., et al., *Donor-Acceptor-Type Heptazine-Based Polymer Networks for Photocatalytic Hydrogen Evolution.* Energy Technology, 2016. **4**(6): p. 744-750.
6. Hosseinzadeh, G., et al., *Unfolding of insulin at the surface of ZnO quantum dots*. Int J Biol Macromol, 2016. **86**: p. 169-76.
7. Xu, H., J. Gao, and D. Jiang, *Stable, crystalline, porous, covalent organic frameworks as a platform for chiral organocatalysts.* Nat Chem, 2015. **7**(11): p. 905-12.
8. Kandambeth, S., et al., *Construction of crystalline 2D covalent organic frameworks with remarkable chemical (acid/base) stability via a combined reversible and irreversible route.* J Am Chem Soc, 2012. **134**(48): p. 19524-7.